



Milankovic Pseudo-cycles Recorded in Sediments and Ice Cores Extracted by Singular Spectrum Analysis

Fernando Lopes¹, Pierpaolo Zuddas², Vincent Courtillot¹, Jean-Louis Le Mouél¹, Jean-Baptiste Boulé³,
Alexis Maineult², Marc Gèze⁴

¹Institut de Physique du Globe, Paris University, Paris 75005, France

²Sorbonne Université, CNRS, EPHE, UMR 7619 METIS, 75005 Paris, France

³Genome Structure and Instability Laboratory, CNRS UMR 7196, INSERM U1154, Muséum national d'Histoire naturelle, Alliance Sorbonne Université, 75005 Paris, France

⁴Centre de Microscopie et d'Imagerie Numérique, Muséum National d'Histoire Naturelle, Paris, France, Muséum national d'Histoire naturelle, Alliance Sorbonne Université, 75005 Paris, France

Correspondence to: Vincent Courtillot (courtil@ipgp.fr)

Abstract. Milankovic cycles describe the changes in the Earth's orbit and rotation axis and their impact on its climate over thousands of years. Singular Spectrum Analysis (**SSA**) is a signal processing method that is best known for its ability to find and extract pseudo-cycles in complex signals. In this short paper, we propose to apply it to three time series that have been proposed as geological reference time scales, in order to retrieve, compare and identify their Milankovic periodicities: (1) LR04, a stack of Plio-Pleistocene benthic microfossil records (Lisiecki and Raymo, 2005), (2) the CO₂ and CH₄ records from the Vostok ice core (Petit et al, 1999) and (3) the long-term orbital solution La04 for the insolation of Laskar et al (2004). The Vostok CO₂ and CH₄ series share the first 7 SSA components, three main ones (98, 104, 39 kyr), and four smaller ones (18, 22, 65, 180 kyr). CO₂ displays a component at 28kyr and a doublet at 61 and 62 kyr. CH₄ displays a doublet near 50 kyr. 18/22 kyr is a precession doublet, 62 kyr an insolation component, and 95/105 kyr an insolation/eccentricity doublet. The 49/50 kyr doublet in CH₄ is not found in the orbital model. The **SSA** results for the La04 orbital solution are in excellent agreement with the values obtained by Laskar et al (2004). Four **SSA** components of *obliquity* are almost identical (rounded figures are 41, 54, 29 and 39 kyr). As far as *eccentricity* is concerned, the first five components are 404, 95, 124, 99, and 132 kyr. The next components are not found in our list of components for eccentricity, but they are in the SSA of *insolation*, at 2338, 970, 488 and 684 kyr. With more than 20 components, the LR04 stack is the richest series. In order of decreasing amplitude, one encounters 41, 95 and 75 kyr components. Next are smaller 39.5 and 53.6 kyr components, and a 22.4 kyr component. One recognizes one of the two main precession components, the doublet of obliquity components, a line at 47.4 kyr that is not found in any of the other spectra, and a doublet at 53.6 and 55.7 kyr, corresponding to the line at 54 kyr found in all four orbital quantities. Next comes a line at 63.6 kyr that may correspond to a line in insolation, CH₄ and CO₂. Then come components from eccentricity variations at 75.2, 94.5, 107.2, 132.1, 198.6 and 400.9 kyr. The remaining components of LR04 show up in La04. The “elusive ~200 kyr eccentricity cycle” of Hilgen et al (2020) is actually present in all three series, in the La04 orbital model as a 195±6 kyr component of eccentricity and in LR04 as a 198.6±5.6 kyr component. Finding not only the main expected Milankovic periodicities but also many “secondary” components with much smaller amplitudes



gives confidence in our iterative SSA method (**iSSA**), on the quality of the La04 model and on the remarkable LR04
35 sedimentary stack, with more than 15 “Milankovic periods”.

1 Introduction

As the geosciences developed in the 19th century, the measure of time at a geological scale became an essential and often controversial topic. As paleontology, sedimentology and stratigraphy amassed information on past forms of life and sedimentary rock formations, a geological time scale of global significance emerged, primarily based on successions of fossil
40 assemblages (Harland et al, 1964). At the turn of the 19th to 20th centuries, the discovery of radiometric dating allowed for the first time the measurement of absolute time (Strutt, 1906; Pigot, 1928). All along the 20th century, pairs of isotopes were added to the toolbox, allowing geologists to explore deeper time with increasing resolution (Wasserburg et al., 1964, 1969). From the 1960s on, the confirmation of the reality of magnetic reversals, as the plate tectonics revolution took place, led to the determination of a reversal time scale (Cande and Kent, 1995). A series of numerical geologic time scales were built and
45 published over the following decades, blending the fossil and magnetic records, with paleontological and magnetic polarity “tie points” anchored on multiple radiometric age determinations (“golden spikes”). The resolution of the best radiometric ages (often performed on volcanic ash layers) was an achievement but did not in general exceed 1% of the age (i.e. 10 kyr at 1 Myr) and involved hypotheses on sedimentation rate (and disintegration constants of isotope pairs).

Rhythmic sedimentary cycles (alternating series of layers such as limestone and marl repeated tens of times and more), that
50 had for long been observed but left unexplained, became an extremely active topic of research in the 1980s as they were interpreted to reflect orbitally induced climate oscillations (Schwartzacher, 1987, 1993; Berger, 1988). With recognition of the validity of Milankovic's ideas, geologists collaborated on the construction of astronomical time-scales. This peaceful race is still going on, leading to unprecedented precision (a fraction of a 20,000 yr precession cycle back to tens of millions of years, or less than 1 per mil).

55 In this paper, we use iterative Singular Spectrum Analysis (**SSA**, e.g. Golyandina et Zhigljavsky, 2013) to determine and compare the (periodical or quasi-periodical) spectral components of three time series, each of a different nature, that have been proposed as reference time scales or used for their construction: a stack of Plio-Pleistocene benthic microfossil records (Lisiecki and Raymo, 2005), the CO₂ and CH₄ records from the famous Vostok ice core (Petit et al, 1999) and the long-term numerical solution for the insolation of Laskar et al (2004).

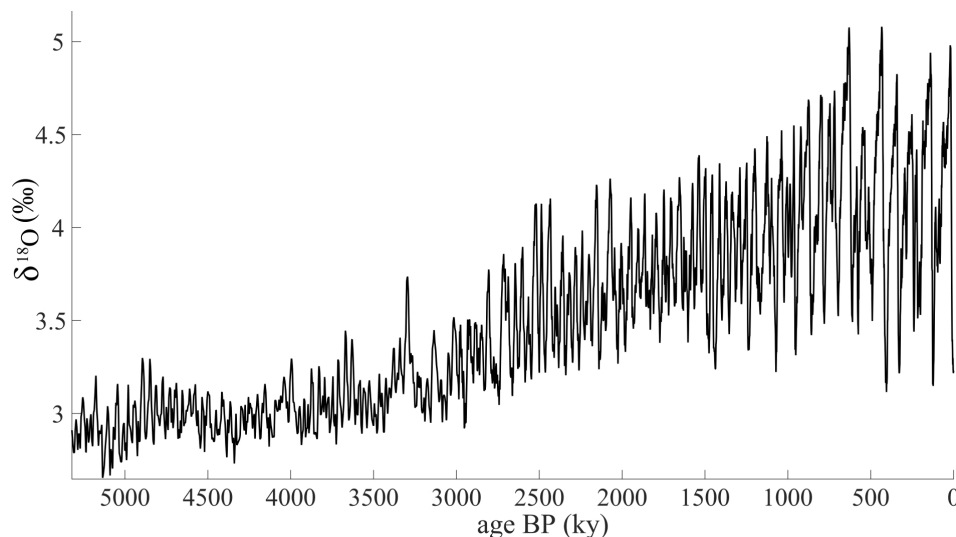
60 We describe the main features of the three series in section 2, compute their SSA components in section 3 and in particular list the periods and quasi-periods of the main components (note: in the present study, **SSA** was able to extract up to 75 cycles; we have limited our discussion and figures to the first ten to twenty, depending on which series is analyzed - see Table 01). We discuss the similarities and differences between the sets of periods and their possible origins in section 4 and then conclude in section 5.



65 2 Data

In this section, we describe the sources and main features of the three time series (actually 8 series from three sources) we analyze with SSA in the next section.

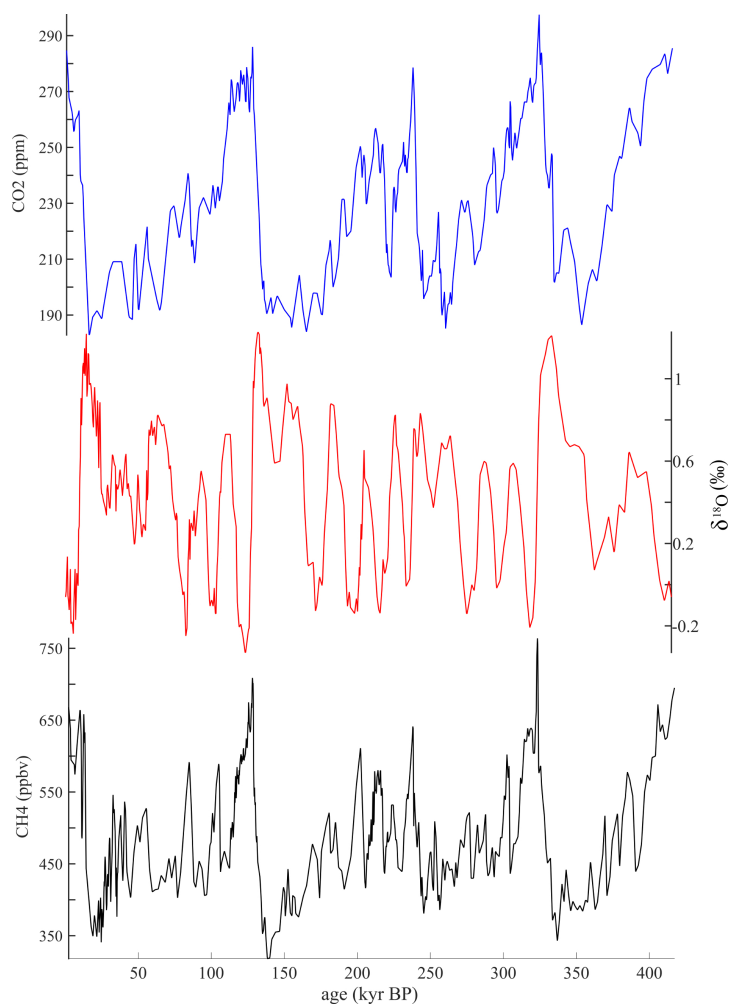
2.1 The Plio-Pleistocene benthic stacked record (Lisiecki and Raymo, 2005)



70

Figure 1: The global benthic stack LR04 back to 5Myr from Lisiecki and Raymo (2005)

Lisiecki and Raymo (2005) present a 5 Myr benthic stack (LR04) that they propose as a paleo-oceanographic type section (Figure 1). It contains 38,229 individual measurements from 57 globally distributed sites. This is archived at <https://www.ngdc.noaa.gov/paleo-search/study/5847>. The $\delta^{18}\text{O}$ are measured on calcite microfossils of foraminifera, for which they are functions of global ice volume and salinity. The alignment of individual profiles is evaluated by eye and adjusted to paleomagnetic reversals and biostratigraphic data. Lisiecki and Raymo (2005) align their stack to a simple model of ice volume, taking into account the average sedimentation rate of the 57 sediment cores in their stack. The top 22 kyr are correlated with a reference ^{14}C -dated benthic record. The 22-120 kyr stack is aligned to the high resolution record from site MD95-2042, itself dated by millennial features of the ratio planktonic to ice from the GRIP ice core. The U-Th dating of coral terraces is used. The tuning target is a non-linear model of ice volume forced by the 21 June insolation at 65°N from the Laskar et al (1993) orbital solution. The above short description is not sufficient for the reader to reconstruct the whole



85 Figure 2: The concentrations of CH₄ (black) and CO₂ (blue) and δ¹⁸O (red) down the Vostok ice-core back to 400 kyr from Petit et al (1999).

process; it is just intended to show that the data we analyze have gone through a rather long and complex suite of scalings. Lisiecki and Raymo (2005) state that the largest uncertainties can shift the age model by 5 kyr at 5 Myr.



90

2.2 The $\delta^{18}\text{O}$, CO_2 and CH_4 histories of the past 420,000 years from the Vostok ice core (Petit et al, 1999)

The Vostok ice core in Antarctica (78°S , 106°E) gave access to a number of paleoclimate series (Petit et al, 1999), among which (paleo-) atmospheric concentrations in CO_2 and CH_4 found to be closely correlated with Antarctic temperature. The record extends to 400 kyr at 3310m depth. Some data are shown in Figure 2; they can be accessed at
 95 <https://www.ncdc.noaa.gov/paleo-search/?dataTypeId=7>. The $\delta^{18}\text{O}$ of (atmospheric) O_2 reflects changes in global ice volume and in the hydrological cycle.

As explained by Petit et al (1999), a glaciological timescale for the top 100 kyr of the core was established by Lorius et al (1983), combining an ice-flow and an accumulation model. Robin (1977) had found a strong correlation between precipitations and temperature in Antarctica. This physics based chronology was extended by Jouzel et al (1993), who called
 100 it the Extended Glaciological Timescale (EGT), and again by Petit et al (1999) to derive GT4 as their primary chronology. They estimated the accuracy of GT4 to be better than 10 kyr for most of the record; it never differed by more than 4 kyr from the orbitally tuned timescale of Waelbroeck et al (1995). Using ^{10}Be , Raisbeck et al (1987) found ages differing by no more than 5 kyr from the EGT. Spectral analysis of their records led Petit et al (1999) to emphasize the dominance of the 100 kyr cycle for CO_2 and CH_4 but not for atmospheric . They also noted a strong signature of the 40 and 20 kyr periodicities.

105

2.3 A long-term numerical solution for the insolation quantities of the Earth (Laskar et al, 2004)

The model of Laskar et al (2004) is a major step (among a large series of models by Jacques Laskar and colleagues) in building solutions computed from astronomy, taking into account changes in the orientation of the Earth's rotation axis, which results in variations of insolation on Earth and thus leading to climate change. In that paper, the authors recall the
 110 history of successive improvements and standstills in computing the secular variations of the Earth's orbital elements. Starting with the names of Lagrange, Laplace and some less famous but important contributors such as Pontécoulant, Agassiz, Adhémar, Croll, Pilgrim, Laskar et al (2004) highlight the names of Milankovic (1941) for the theory, and Hays et al (1976) for observations of the records over the past 500 kyr.

Laskar et al. (2004) have solved the astronomical equations for the insolation quantities on Earth back to -250 Myr.
 115 In Laskar et al's (2004) terms, *"this solution has been improved with respect to La93 (Laskar et al. 1993) by using a direct integration of the gravitational equations for the orbital motion, and by improving the dissipative contributions, in particular in the evolution of the Earth–Moon System. The orbital solution has been used for the calibration of the Neogene period (Lourens et al. 2004)."*

Laskar et al's (2004) orbital model comprises all 9 planets of the solar system. It involves post-Newtonian general
 120 relativity corrections due to the Sun and the leading coefficients of the gravitational potential of Earth and the Moon, and tidal dissipation in the Earth-Moon system. Numerical integration is an important part of the computations. We will be



particularly interested in Laskar et al.'s (2004) Tables 6 and 7, respectively giving the 20 leading frequency components of eccentricity and obliquity. The time series of insolation, eccentricity, obliquity and precession are found on the IMCCE (Institut de Mécanique Céleste et du Calcul des Ephémérides) site at
 125 <http://vo.imcce.fr/insola/earth/online/earth/online/index.php>.

3 Singular Spectrum Analysis

We now submit the three series described in the previous section to Iterative Singular Spectrum Analysis (iSSA, see Golyandina and Zhigljavsky, 2013). The reason why we have thought of applying SSA (that is less common than the Fourier or Wavelet transforms) to these time series is that we have recently successfully applied the method to a number of geophysical and heliophysical time series. We have explained the method in a number of papers (Lopes et al., 2017, 2021; Le Mouél et al., 2020a). A symmetric matrix is decomposed following Golub and Kahan's (1965) Singular Value Decomposition (SVD). The "constant descent" diagonal (Hankel) matrix has column vectors that are pieces of the signal under analysis (see Golyandina and Zhigljavsky, 2013).

For instance, oscillations (pseudo-cycles) of 80, 60, 20 and 11 yr appear in sunspots (Gleissberg, 1944; Coles et al., 1980; Charvatova and Strestik, 1991; Usoskin, 2017; Le Mouél et al., 2020b; Courtillot et al., 2021) as well as in a number of terrestrial phenomena (Wood and Lovett, 1974; Mörth and Schlamminger, 1979; Schlesinger and Ramankutty, 1991; Lau and Weng, 1995; Scafetta, 2010; Courtillot et al., 2013; Scafetta, 2016; Lopes et al., 2017; Le Mouél et al., 2019a; Le Mouél et al., 2019b; Le Mouél et al., 2020a; Scafetta et al., 2020; Lopes et al., 2021; Scafetta, 2021), in particular sea-level
 140 (Jevrejeva et al., 2006; Chambers et al., 2012; Merrifield et al., 2012; Chen et al. 2012; Le Mouél et al., 2021). They can be compared to the commensurable periods of the Jovian planets acting on Earth and Sun as proposed by Mörth and Schlamminger (1979): a combination of the revolution periods of Neptune (165 yr), Uranus (84 yr), Saturn (29 yr) and Jupiter (12 yr) and several commensurable periods (see f.i. Table 1 in Lopes et al, 2021 and Courtillot et al. (2021) for the action of the Jovian planets on sunspots).

145

3.1 SSA of the long-term numerical solution for insolation of Laskar et al. (2004)

The SSA periods or quasi-periods of eccentricity, precession, obliquity and insolation computed with the Laskar et al (2004) La04 orbital model are listed in the last four columns of Table 1, together with their uncertainties and share of the total signal variance. The uncertainties are estimated to be the half-width at half maximum (peak) value of the Fourier transform of the relevant SSA component (e.g. Lopes et al, 2021). The components are listed in Table 1 in increasing order of the period.



	Lisiecki et Raymo (2005)	Petit et al. (1999)		Laskar et al. (2004)			
		CH ₄	CO ₂	Insolation	Eccentricity	Precession	Obliquity
155	22.38 ± 0.12 (1.2%)	18.80 ± 0.71 (2.0%) 21.68 ± 0.80 (1.1%) 24.22 ± 0.89 (2.8%)	17.99 ± 0.55 (2.4%) 22.17 ± 0.73 (1.6%) 28.47 ± 1.22 (5.4%)			18.94 ± 0.04 (18.6%) 22.35 ± 0.06 (26.0%)	28.85 ± 0.10 (11.3%)
160	35.40 ± 0.16 (0.4%) 39.52 ± 0.22 (1.3%) 40.98 ± 0.23 (21.2%) 47.44 ± 0.25 (0.8%)	39.00 ± 2.15 (12.3%) 48.63 ± 3.45 (0.8%)	38.92 ± 2.41 (7.7%) 60.84 ± 10.27 (5.2%) 62.79 ± 9.95 (2.1%)	54.03 ± 0.35 (0.2%) 62.35 ± 0.48 (0.2%)	54.94 ± 0.36 (0.9%) 76.88 ± 0.71 (0.8%)	53.95 ± 0.36 (2.5%)	39.53 ± 0.18 (10.9%) 40.91 ± 0.21 (54.9%) 53.59 ± 0.35 (19.2%)
165	53.64 ± 0.38 (1.3%) 55.69 ± 0.77 (0.01%) 63.62 ± 1.03 (0.04%) 69.12 ± 0.64 (0.2%) 70.87 ± 0.85 (5.3%) 75.19 ± 2.17 (0.3%) 83.34 ± 1.23 (0.01%) 90.85 ± 0.94 (18.5%) 94.50 ± 2.95 (0.7%)	50.26 ± 4.47 (1.0%) 65.65 ± 6.96 (3.4%)	97.87 ± 12.92 (19.72%)	87.89 ± 0.98 (0.1%) 94.95 ± 1.23 (22.3%) 99.15 ± 1.25 (10.7%) 105.93 ± 2.69 (0.9%) 117.95 ± 1.63 (1.6%) 123.92 ± 3.21 (11.8%) 131.36 ± 2.27 (6.7%)	95.15 ± 1.11 (20.8%) 99.49 ± 1.26 (6.0%) 106.49 ± 1.22 (1.4%) 117.78 ± 1.62 (0.2%) 124.46 ± 4.06 (10.6%) 131.92 ± 2.17 (3.3%) 140.00 ± 2.53 (0.1%)		
170	107.16 ± 2.70 (0.7%) 132.08 ± 2.54 (0.3%) 147.60 ± 3.10 (0.02%) 161.54 ± 3.04 (0.3%) 178.03 ± 3.34 (0.3%)	98.99 ± 13.16 (13.5%) 104.36 ± 18.66 (4.6%)	104.23 ± 19.40 (10.1%) 187.65 ± 71.50				
175	198.64 ± 5.57			405.35 ± 20.18 488.00 ± 30.97 684.52 ± 60.07 970.28 ± 110.67 2338.05 ± 715.29	195.00 ± 6.13		
180							

Table 1: Synthesis of periods and quasi periods (components) extracted by iSSA from (from left to right) the LR04 stack of profiles from Lisiecki and Raymo (2005), the CH₄ and CO₂ concentrations down the Vostok ice-core from Petit et al (1999), and the insolation, eccentricity, precession and obliquity of the La04 orbital solution of Laskar et al (2004). The contribution to the variance of each component is printed in bold between parentheses.

Precession starts with a doublet at 22.3 and 18.9 kyr (respectively 26.0 and 18.6 % of the signal variance) and has a 3rd component at 53.9 kyr (2.5% of the s.v.) for a total of 47% of the s.v.

Obliquity starts with a doublet at 40.9 and 39.5 kyr (respectively 54.9 and 10.9 % of the s.v.), followed by a large component at 53.6 kyr (19.2% of the s.v.) and one at 28.8 kyr (11.3% of the s.v.). Taken together these 4 components amount to 96.3% of the s.v.

Eccentricity has the richest spectrum. Twelve components are listed in Table 1, the main one at 404 kyr (34.8% of the s.v.), then at 95 kyr (20.8%), 124 kyr (10.6%), 99 kyr (6.0%), 132 kyr (3.3%) and 106 kyr (1.4%). Other components are well determined and identified at below 1% of the s.v. Taken together, the first six components amount to 76.9% of the signal variance.



Insolation is dominated by the spectrum of eccentricity, with which it shares 8 components. The first five components have essentially identical values and similar rank and shares of s.v. The sixth one at 970 ± 110 kyr (2.8% of s.v.) is ill determined but is important; it does not appear in the SSA of eccentricity. Eccentricity and insolation also share components at 54, 106 and 118 kyr, but below 1% contribution to s.v. Some components are found only in eccentricity (77, 140, 195, 346 kyr) or insolation (62, 88, 488, 684, 2338 kyr, the last three with large uncertainties).

3.2 SSA of the Plio-Pleistocene benthic stacked record

The periods or quasi-periods of the Plio-Pleistocene benthic stacked record of Lisiecki and Raymo (2005) are listed in the first column of Table 1, together with their uncertainties and share of the total signal variance. The components are listed in Table 1 in increasing order of the period. In order of decreasing amplitude, one encounters a 41 kyr component (21.2% of the s.v.), a 95 kyr component (18.5% of the s.v.) and a 75 kyr component (5.3% of the s.v.). Next at 1.3% are a 39.5 and 53.6 kyr component, and at 1.2% a 22.4 kyr component. All other components are below 1% of the s.v.

3.3 SSA of the $\delta^{18}\text{O}$, CO_2 and CH_4 histories from the Vostok ice core

The SSA periods or quasi-periods of the CO_2 and CH_4 histories of the past 420,000 years from the Vostok ice core (Petit et al, 1999) are listed in the second and third columns of Table 1. The two series share the first three components, sometimes with a slight exchange of rank (98, 104, 39 kyr), and four others (18, 22, 65, 180 kyr), the longest periods having large uncertainties. CO_2 displays a component at 24 kyr (5.4% of the s.v.) and a doublet at 61 and 62 kyr. CH_4 displays a component at 28 kyr (2.8% of the s.v.) and a doublet near 50 kyr.

4 Comparisons and Discussion

We can first compare the results of the SSA of the La04 orbital solution with respect to the actual values obtained by Laskar et al (2004).

Four SSA components of *obliquity* are almost identical (to 0.3 to 2%) with those listed in Laskar et al's (2004) Table 7: 40.9, 53.6, 28.9 and 39.5 kyr vs 41.0, 39.6, 53.7 and 29.8 kyr. We note that the order of amplitudes is not exactly the same. This is because SSA finds only one component when La04 has many closely spaced multiplets (9 for the 41 kyr component, 5 for the 29 kyr component,...).

In their Table 7 Laskar et al (2004) list the 20 frequency components of *eccentricity* on the [-15 Myr, +5 Myr] time interval. They also indicate the planetary conjunctions and resonances to which these periods correspond. A comparison of Table 1 (column 5) and Laskar et al's (2004) Table 6 shows almost perfect agreement: in order of decreasing share of variance the first five components are 404, 95, 124, 99, and 132 kyr (Table 1, this paper) vs 405, 95, 124, 99, and 131 kyr (Laskar et al, 2004). Uncertainties for our values are on the order of 1 to 5% and are probably overestimates, the agreement of the list of frequencies being often better. The next components (6, 7, 9 and 10) are not found in our list, but they are in the



SSA of *insolation* (column 4): 2338, 970, 488 and 684 kyr vs 2373, 978, 486 and 688 kyr (with uncertainties on the order of 10%). The first five components of eccentricity and insolation contain respectively 75 and 89% of the series total variance.

Next, we encounter components 8, 11 to 15 and 17 to 20 (all still in kyr): 106, 99 (a doublet with component 4), 77, 132, 106 (a doublet with component 8), 118, 124, 55, 95 (a doublet of component 2) and 345 kyr vs 105, 101, 77, 134, 103, 118, 127, 55, 97 and 346 kyr.

We find 3 components that are not in the La04 list at 109, 140 and 195 kyr. Eccentricity has the main influence on insolation. Indeed, they both comprise 12 identical periods (or quasi periods, see later). We have also seen that 4 additional components are in La04 insolation and eccentricity, but not in our decomposition of eccentricity. Components at 62 and 88 kyr are found in our analysis of La04 insolation but not in eccentricity.

We note that the 195 ± 6 kyr could well correspond to the “elusive ~200 kyr eccentricity cycle” claimed to have been revealed in paleoclimate records for the first time by Hilgen et al (2020). We will soon see that this cycle is present both in the CO₂ record of Petit et al (1999) and more precisely in the LR04 stack of Lisiecky and Raymo (2005).

The CH₄ and CO₂ records of Petit et al (1999) share 7 components. These include the precession doublet at 18 and 22 kyr, the obliquity doublet at 39 and 41 kyr, an insolation component at 62 kyr, an insolation/eccentricity doublet at 95 and 105 kyr and the “elusive” ~200 kyr component. CO₂ has a component at 28.5 kyr (not found in CH₄ but present in obliquity); CH₄ has a component at 24.2 kyr (not found in CO₂ or any other series), and a doublet at 48.6 and 50.3 kyr (not found in the orbital model). The sums of the nine first components of CH₄ and CO₂ (those in excess of 1%) carry 46 and 48% respectively of the series variances.

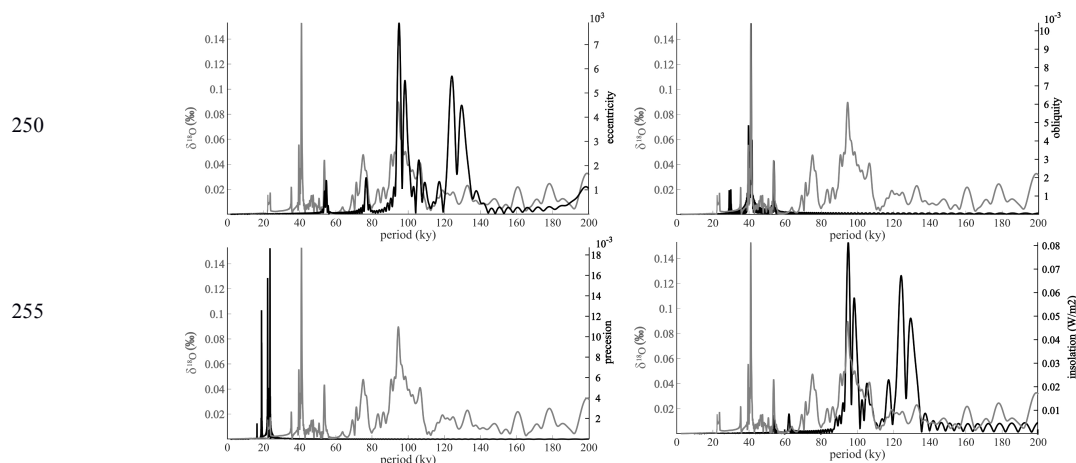
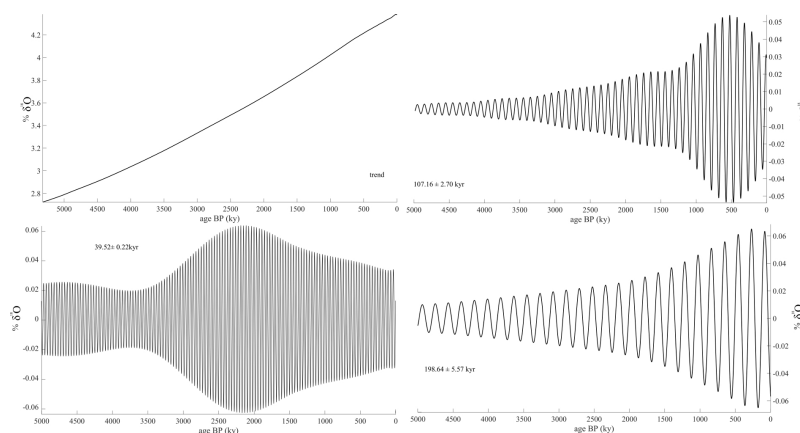


Figure 3: The theoretical (orbital model La04) spectra of eccentricity (grey curve, upper left), obliquity (grey curve, upper right), precession (grey curve, lower left), and insolation (grey curve, lower right) compared to (superimposed on) the observed sedimentary spectrum (black curves in all frames).



265 Last but not least, the LR04 stack of Lisiecki and Raymo (2005). With more than 20 components, the LR04 stack is
 the richest series. From shorter to longer period (and pseudo-period) components, one recognizes in the first column of Table
 1 one of the two main precession components (22.4 kyr), the doublet of obliquity components (39.5 and 41.0 kyr), a line at
 47.4 kyr that is not found in any of the other spectra, a doublet at 53.6 and 55.7. This corresponds to the line at 54 kyr found
 in all four orbital quantities. Then comes a line at 63.6 kyr that may correspond to a line in insolation, CH₄ and CO₂. Then
 come components that must come from eccentricity variations at 75.2, 94.5, 107.2, 132.1, 198.6 and 400.9 kyr (viz La04
 270 values of 76.9, 95.1, 106.5, 131.9, 195.0 and 404.5 kyr). The remaining components show up in La04 but not in any other
 series we analyzed unless tentatively suggested in a parenthesis: 35.4 kyr, 47.4 (maybe in CH₄ a member of the 48.6 and 50.3
 kyr doublet), a 69.1 plus 70.9 kyr doublet, 83.3, 90.8, 147.6, 161.5 and 293.3 kyr. The sum of the first six components of
 LR04 (those in excess of 1%) totals 49% of the signal variance.

275 In Figure 3, we display the reconstructed spectrum of the LR04 benthic stack and compare it to the full spectra of the
 separate parameters of the La04 orbital model. The LR spectrum is shown as a brown curve in all four frames of Figure 3
 and the spectra from La04 are superimposed in red for the eccentricity (top left), in green for obliquity (top right), in blue for
 precession (bottom left) and in purple for insolation (bottom right). The spectral components of obliquity and precession are
 fully recorded but take place over a narrow period range. The 80 to 110 kyr parts of the eccentricity (and insolation)
 280 spectrum are well reflected in the sedimentary spectrum, but the 110 to 140 kyr part is present but strongly attenuated. Linear
 models are not suitable to describe these relationships and therefore temperature (a function of insolation) is not linearly
 related to isotopic ratios ($\delta^{18}\text{O}$).

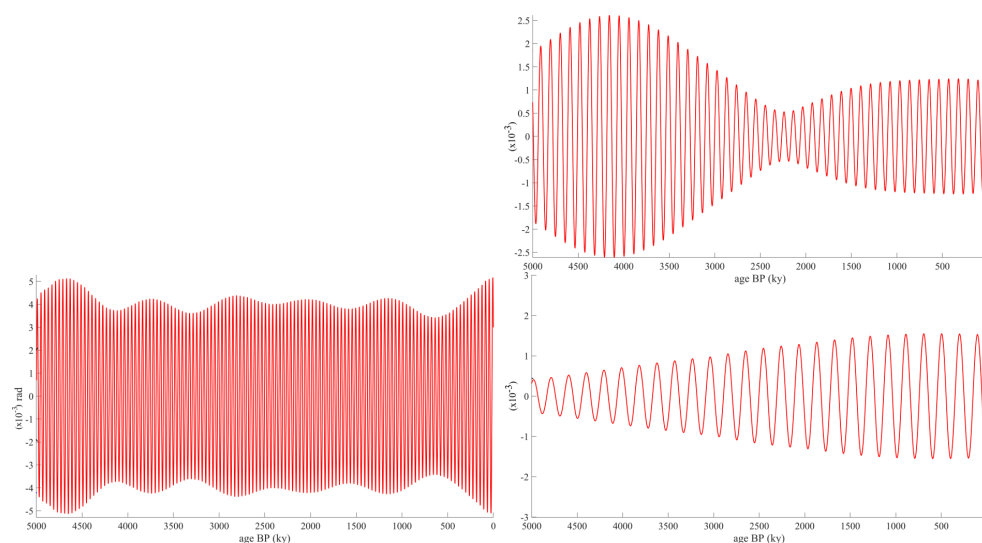




295 Figure 4 from left to right and top to bottom: the trend (SSA component 0) of the , the 107 kyr SSA component associated to
 insolation, the 39 kyr SSA component associated to obliquity and the 198 kyr SSA component associated to eccentricity, all
 from sedimentary stack LR04.

The SSA analysis of from the LR04 stack of sedimentary cores, and CH₄ and CO₂ from the Vostok ice-core of course
 300 confirms many earlier findings on the forcing of proxies of climate by orbital dynamics. SSA allows one to reconstruct these
 series very well. An advantage of the SSA method over the Fourier or wavelet analyses is that individual components can
 vary in frequency and be modulated in amplitude and phase. This is illustrated by Figure 4, a selection of SSA components.
 From left to right and top to bottom: the trend (component 0) of the from the sedimentary stack LR04, the 107 kyr
 component of insolation, the 39 kyr component associated to obliquity and the “elusive” (Hilgen et al, 2020) 198 kyr
 305 component associated to eccentricity. The SSA components have a finite width, and are more or less strongly modulated.
 They vary considerably in scales of amplitudes and can be quasi-periodical and not perfect sinusoids.. Figure 5 shows the
 corresponding components of orbital model La04. The shapes of the modulation envelopes of corresponding components are
 rather different. This may lead one to the response functions of the various components, which is beyond the purpose of the
 present paper.

310



325

Figure 5 from left to right and top to bottom: the 107 kyr SSA component of insolation, the 39 kyr SSA component of
 obliquity and the 198 kyr SSA component of eccentricity, all from orbital model La04.



330 5 – Summary and Conclusion

The main goal of this paper has been to check the efficiency of Singular Spectrum Analysis in determining the spectral components of three time series of a significantly different nature, three time series that have been proposed as reference time scales or used for their construction. They are a stack of Plio-Pleistocene benthic microfossil records (Lisiecki and Raymo, 2005), the CO₂ and CH₄ records from the Vostok ice core (Petit et al, 1999) and the long-term numerical solution for the insolation of Laskar et al (2004). We have submitted the three series to Iterative Singular Spectrum Analysis (iSSA, Golyandina and Zhigljavsky, 2013); we have explained the method in several papers (Lopes et al., 2017, 2021; Le Mouél et al., 2020a) and we have successfully applied it to a number of geophysical and heliophysical time series.

For instance, oscillations (pseudo-cycles) of 80, 60, 20 and 11 yr appear in sunspots as well as in a number of terrestrial phenomena, in particular sea-level (see references in section 3). These values belong to a well defined family of commensurable periods of the Jovian planets that act on the Earth and the Sun (Mörth and Schlamminger, 1979): a combination of the revolution periods of Neptune (165 yr), Uranus (84 yr), Saturn (29 yr) and Jupiter (12 yr) and several commensurable periods (see f.i. Table 1 in Lopes et al, 2021 and Courtillot et al. (2021) for the action of the Jovian planets on sunspots).

(1) The Vostok ice core in Antarctica (Petit et al, 1999) gives access to atmospheric paleo-concentrations in CO₂ and CH₄, that are closely correlated with Antarctic temperature. The record extends to 420 kyr. A glaciological timescale has been established that combines an ice-flow and an accumulation model. This physics based chronology was extended to derive chronology GT4 with an estimated accuracy better than 10 kyr for most of the record. The SSA periods or quasi-periods of the CO₂ and CH₄ histories are listed in the second and third columns of Table 1. The two series share the first 7 components, three main ones (98, 104, 39 kyr), and four smaller ones (18, 22, 65, 180 kyr). CO₂ displays a component at 28kyr and a doublet at 61 and 62 kyr. CH₄ displays a doublet near 50 kyr. 18/22 ky is a precession doublet, 62 kyr an insolation component, and 95/105 kyr an insolation/eccentricity doublet. The 49/50 kyr doublet in CH₄ is not found in the orbital model.

(2) The Laskar et al. (2004) solution of the astronomical equations for insolation back to –250 Myr. The orbital model comprises all 9 planets of the solar system. Laskar et al's (2004) Tables 6 and 7, give the 20 leading frequency components of eccentricity and obliquity. Table 1 gives our SSA determinations of the components. *Precession* starts with a doublet at 22.3 and 18.9 kyr and has a 3rd component at 53.9 kyr. *Obliquity* starts with a doublet at 40.9 and 39.5 kyr, followed by a large component at 53.6 kyr and one at 28.8 kyr. *Eccentricity* has the richest spectrum. The main component is at 404 kyr, the next ones at 95, 124, 99, 132 and 106 kyr. Other components are well determined and identified at below 1% of the s.v. *Insolation* is dominated by the spectrum of eccentricity, with which it shares 8 components. The first five components have essentially identical values and similar rank and shares of s.v. The sixth one at 970±110 kyr does not appear in the SSA of



eccentricity. Eccentricity and insolation also share components at 54, 106 and 118 kyr, but below 1% contribution to s.v. Some components are found only in eccentricity (77, 140, 195, 346 kyr) or insolation (62, 88, 488, 684, 2338 kyr, the last three with large uncertainties).

Our SSA results of the La04 orbital solution are in excellent agreement with the values obtained by Laskar et al (2004), with a few interesting differences (that are part of the tests of the SSA method). Four SSA components of *obliquity* are almost identical (to better than 2%): rounded figures are 41, 54, 29 and 39 kyr. As far as *eccentricity* is concerned, the first five components are 404, 95, 124, 99, and 132 kyr. The next components (6, 7, 9 and 10) are not found in our list, but they are in the SSA of *insolation*: 2338, 970, 488 and 684 kyr.

Next, we encounter components 8, 11 to 15 and 17 to 20 (all still in kyr): 106, 99 (a doublet with component 4), 77, 132, 106 (a doublet with component 8), 118, 124, 55, 95 (a doublet of component 2) and 345 kyr. We find 3 components that are not in the La04 list at 109, 140 and 195 kyr. *Eccentricity* has the main influence on *insolation*. Indeed, they both comprise 12 identical periods (or quasi periods). We have also seen that 4 additional components are in La04 *insolation* and *eccentricity*, but not in our decomposition of *eccentricity*. Components at 62 and 88 kyr are found in our analysis of La04 insolation but not in eccentricity.

(3) The periods or quasi-periods of the Plio-Pleistocene benthic stacked record of Lisiecki and Raymo (2005) are listed in the first column of Table 1. With more than 20 components, the LR04 stack is the richest series. In order of decreasing amplitude, one encounters a 41 kyr component, a 95 kyr component and a 75 kyr component. Next are smaller 39.5 and 53.6 kyr component, and a 22.4 kyr component. All other components are below 1% of the s.v. One recognizes one of the two main precession components (22.4 kyr), the doublet of obliquity components (39.5 and 41.0 kyr), a line at 47.4 kyr that is not found in any of the other spectra, a doublet at 53.6 and 55.7. This corresponds to the line at 54 kyr found in all four orbital quantities. Next comes a line at 63.6 kyr that may correspond to a line in insolation, CH₄ and CO₂. Then come components from eccentricity variations at 75.2, 94.5, 107.2, 132.1, 198.6 and 400.9 kyr. The remaining components of LR04 show up in La04 but not in any other series we analyzed.

Hilgen et al (2020) claim to have identified for the first time in paleoclimate records an “elusive ~200 kyr eccentricity cycle”. This cycle is possibly already present in the CO₂ and CH₄ Vostok cores, but with a very large uncertainty (187.6±71.5 and 178.4±60.6 kyr, respectively). It is present in the La04 orbital model as a 195±6 kyr component of eccentricity. And finally it is found as a 198.6±5.6 kyr component of LR04 (all values from Table 1)

It has long been known that Milankovic cycles could be identified in sediment and ice cores as well (Jouzel et al., 2007; Loulergue et al., 2008; Cheng et al., 2016), with leading terms with periods 19 to 23 kyr due to equinoctial precession, 41 kyr due to the obliquity variations of the Earth’s axis, and 95 to 100 kyr for variations in eccentricity of the Earth’s orbit. As is the case for Earth tides, the fact that one deals with celestial objects in rotation and revolution on slowly variable orbits, influencing each other, makes “harmonic” periods appear in the solutions obtained with the equations of celestial mechanics (Laplace, 1799), in addition to the main periods recalled above. Many of these “secondary” components have much smaller amplitudes. Yet, if they can be observed they give confidence in the theory and models built from it. In that respect, the



395 identification by SSA of more than 15 “Milankovic periods” in the LR04 sedimentary stack and 9 in the Vostok core is
important.

The rich list of SSA (Milankovic) components in the sedimentary stack suggests that benthic foraminifera in marine
sediments are particularly appropriate to study paleoclimates. This may be related to the fact that benthic sections are
selected to be located in areas with stable environments, linked to water depth and the pattern of large oceanic currents.

400



Author contribution: FL, JLLM, VC, PZ conceived the study, FL did most of the computing, FL, VC and JLLM wrote the paper, JBB, AM and MG contributed to the discussion.

405 **Competing interests:** The authors declare that they have no conflict of interest.

References

- Adhémar, J. A.: Révolutions de la mer, déluges périodiques, Vol. 1, Lacroix-Comon, Paris, 1860.
- Barnola, J. M., Raynaud, D. Y. S. N., Korotkevich, Y. S., and Lorius, C.: Vostok ice core provides 160,000-year record of atmospheric CO₂, *Nature*, 329(6138), 408-414, 1987.
- 410 Berger, A. (1988). Milankovitch theory and climate. *Reviews of geophysics*, 26(4), 624-657.
- Boretti, A.: Analysis of Segmented Sea level Time Series, *Applied Sciences*, 10(2), 625, 2020.
- Cande, S.C., and Kent, D.V.: Revised calibration of the geomagnetic polarity timescale for the Late Cretaceous and Cenozoic, *J. Geophys. Res. Solid Earth*, 100, 6093-6095, 1995.
- Cheng, Hai, R. L. Edwards, A. Sinha, C. Spötl, Liang Yi, Shitao Chen, M. Kelly et al.: The Asian monsoon over the past 640,000 years and ice age terminations, *Nature*, 534, 640-646, 2016.
- 415 Courtillot, V., and Le Mouél, J. L., Time variations of the earth's magnetic field-From daily to secular, *Ann. Rev. Earth and Planet. Sci.*, 16, 389-476, 1988.
- Courtillot, V., Le Mouél, J.L., Kossobokov, V., Gibert, D and Lopes, F.: Multi-Decadal Trends of Global Surface Temperature: A Broken Line with Alternating ~30 yr Linear Segments?, *Atmos. and Clim. Sci*, Vol.3 No.3, Article ID:34080, 8 pages, 2013.
- 420 Courtillot, V., Lopes, F., and Le Mouél, J. L.: On the prediction of solar cycles, *Solar Physics*, 296(1), 1-23, 2021.
- Dansgaard, W.: Comparative measurements of standards for carbon isotopes, *Geochim. Cosmochim. Acta*, 3(5), 253-256, 1953.
- Golyandina, N., and Zhigljavsky, A.: *Singular Spectrum Analysis for time series*, Vol. 120, Berlin, Springer, 2013.
- Harland, W. B., Smith, A. G., & Wilcock, B. (Eds.). (1964). *The Phanerozoic time-scale*. London: Geological Society of London.
- Hilgen, F., Zeeden, C., and Laskar, J.: Paleoclimate records reveal elusive~ 200-kyr eccentricity cycle for the first time, *Global and*
- 425 *Planetary Change*, 194, 103296, 2020.
- Jouzel, J., Barkov, N. I., Barnola, J. M., Bender, M., Chappellaz, J., Genthon, C., ... and Yiou, P.: Extending the Vostok ice-core record of palaeoclimate to the penultimate glacial period, *Nature*, 364(6436), 407-412, 1993.
- Jouzel, Jean, Valérie Masson-Delmotte, Olivier Cattani, Gabrielle Dreyfus, Sonia Falourd, Georg Hoffmann, Benedicte Minster et al.: Orbital and millennial Antarctic climate variability over the past 800,000 years, *Science*, 317, no. 5839, 793-796, 2007.
- 430 Kay, S. M., and Marple, S. L.: Spectrum analysis—a modern perspective, *Proceedings of the IEEE*, 69(11), 1380-1419, 1981.
- Laplace, Pierre Simon.: *Traité de mécanique celeste*, de l'Imprimerie de Crapelet, Paris, 1799.
- Laskar, J., Robutel, P., Joutel, F., Gastineau, M., Correia, A. C. M., and Levrard, B.: A long-term numerical solution for the insolation quantities of the Earth, *Astronomy and Astrophysics*, 428(1), 261-285, 2004.
- Le Mouél, J. L., Lopes, F., and Courtillot, V.: A solar signature in many climate indices, *J. Geophys. Res.: Atmospheres*, 124(5), 2600-
- 435 2619, 2019a.



- Le Mouél, J. L., Lopes, F., Courtillot, V., and Gibert, D.: On forcings of length of day changes: From 9-day to 18.6-year oscillations, *Phys. Earth Planet. Int.*, 292, 1-11., 2019b.
- Le Mouél, J. L., Lopes, F., and Courtillot, V.: Characteristic time scales of decadal to centennial changes in global surface temperatures over the past 150 years, *Earth and Space Science*, 7(4), e2019EA000671, 2019c.
- 440 Le Mouél, J. L., Lopes, F., & Courtillot, V.: Solar turbulence from sunspot records, *Month. Notices Roy. Astr. Soc.*, 492(1), 1416-1420, 2020a.
- Le Mouél, J. L., Lopes, F., and Courtillot, V.: Sea-Level Change at the Brest (France) Tide Gauge and the Markowitz Component of Earth's Rotation, *Journal of Coastal Research*, 37 (4), 683-690, 2021.
- Lisiecki, L. E., and Raymo, M. E. (2005). A Pliocene-Pleistocene stack of 57 globally distributed benthic $\delta^{18}\text{O}$ records. *Paleoceanography*, 20(1), PA1003, doi:10.1029/2004PA001071, 2005.
- 445 Lopes, F., Le Mouél, J. L., and Gibert, D.: The mantle rotation pole position. A solar component, *Comptes Rendus Geoscience*, 349(4), 159-164, 2017.
- Lopes, F., Le Mouél, J. L., Courtillot, V., and Gibert, D.: On the shoulders of Laplace, *Phys. Earth Planet. Int.*, 316, 106693, doi = {10.1016/j.pepi.2021.106693}, 2021.
- 450 Lorius, C., Merlivat, L., Jouzel, J., and Pourchet, M.: A 30,000-yr isotope climatic record from Antarctic ice., *Nature*, 280(5724), 644-648, 1979.
- Lorius, C., Jouzel, J., Ritz, C., Merlivat, L., Barkov, N. I., Korotkevich, Y. S., and Kotlyakov, V. M.: A 150,000-year climatic record from Antarctic ice, *Nature*, 316(6029), 591-596, 1985.
- Loulergue, L., A. Schilt, R. Spahni, V. Masson-Delmotte, T. Blunier, B. Lemieux, J.M. Barnola, D. Raynaud, T. Stocker, and J.
- 455 Chappellaz: Orbital and millennial-scale features of atmospheric CH_4 over the past 800,000 years, *Nature*, 453(7193), 383-386, 2008.
- Milanković, M.: *Théorie mathématique des phénomènes thermiques produits par la radiation solaire*, Faculté des sciences de l'Université de Belgrade, Gauthier-Villard édition, 1920.
- Milankovic, M.: *Canon of insolation of the earth and its application to the problem of the ice ages*, Royal Serbian Academy Press, Cemian, 1-626, 1941.
- 460 Mörner, N. A.: Planetary, solar, atmospheric, hydrospheric and endogene processes as origin of climatic changes on the Earth, In *Climatic changes on a yearly to millennial basis* (pp. 483-507), Springer, Dordrecht, 1984.
- Mörner, N. A.: Solar wind, earth's rotation and changes in terrestrial climate, *Physical Science Int. Journal*, 117-136, 2013.
- Mörth, H. T., and Schlamminger, L.: Planetary motion, sunspots and climate, In *Solar-Terrestrial Influences on Weather and Climate* (pp. 193-207), Springer, Dordrecht, 1979.
- 465 Petit, J. R., Jouzel, J., Raynaud, D., Barkov, N. I., Barnola, J. M., Basile, I., ... and Stievenard, M.: Climate and atmospheric history of the past 420,000 years from the Vostok ice core, Antarctica, *Nature*, 399(6735), 429-436, 1999.
- Piggot, C. S. (1928). Radium and Geology I. *Journal of the American Chemical Society*, 50(11), 2910-2916.
- Raisbeck, G. M., Yiou, F., Bourles, D., Lorius, C., Jouzel, J., and Barkov, N. I.: Evidence for two intervals of enhanced ^{10}Be deposition in Antarctic ice during the last glacial period, *Nature*, 326(6110), 273-277, 1987.
- 470 Raymo, M. E., Oppo, D. W., and Curry, W.: The mid-Pleistocene climate transition: A deep sea carbon isotopic perspective., *Paleoceanography*, 12(4), 546-559, 1997.
- Robin, G. de Q.: Ice cores and climatic change, *Phil. Trans; Roy. Soc; of London, Biological Sciences*, 280.972, 143-168, 1977.



- Scafetta, N.: High resolution coherence analysis between planetary and climate oscillations, *Advances in Space Research*, 57(10), 2121-2135, 2016.
- 475 Scafetta, N.: The complex planetary synchronization structure of the solar system, arXiv preprint arXiv:1405.0193, 2014.
- Scafetta, N., Milani, F., Bianchini, A., and Ortolani, S.: On the astronomical origin of the Hallstatt oscillation found in radiocarbon and climate records throughout the Holocene, *Earth-Science Reviews*, 162, 24-43, 2016.
- Scafetta, N.: Solar Oscillations and the Orbital Invariant Inequalities of the Solar System, *Solar Physics*, 295(2), 1-19, 2020.
- Schwarzacher, W. (1987). The analysis and interpretation of stratification cycles. *Paleoceanography*, 2(1), 79-95.
- 480 Schwarzacher, W. (1993). *Cyclostratigraphy and the Milankovitch theory*. Elsevier.
- Strutt, R. J. (1906). On the distribution of radium in the Earth's crust and on the Earth's internal heat. *Proceedings of the Royal Society of London. Series A, Containing Papers of a Mathematical and Physical Character*, 77(519), 472-485.
- Urey, H. C., & Greiff, L. J.: Isotopic exchange equilibria, *Journal of the American Chemical Society*, 57(2), 321-327, 1935.
- Urey, H. C.: The thermodynamic properties of isotopic substances, *Journal of the Chemical Society (Resumed)*, 562-581, 1947.
- 485 Urey, H. C.: Oxygen isotopes in nature and in the laboratory, *Science*, 108(2810), 489-496, 1948.
- Wasserburg, G. J., MacDonald, G. J., Hoyle, F., & Fowler, W. A. (1964). Relative contributions of uranium, thorium, and potassium to heat production in the Earth. *Science*, 143(3605), 465-467.
- Wasserburg, G. J., Papanastassiou, D. A., Nienow, E. V., & Bauman, C. A. (1969). A programmable magnetic field mass spectrometer with on-line data processing. *Review of Scientific Instruments*, 40(2), 288-295.